Light harvesting vesicular donor–acceptor scaffold limits the rate of charge recombination in the presence of an electron donor

Rijo T. Cheriya, Ajith R. Mallia and Mahesh Hariharan*

School of Chemistry, Indian Institute of Science Education and Research Thiruvananthapuram (IISER-TVM), CET Campus, Sreekaryam, Thiruvananthapuram, Kerala 695 016, Fax: (91)-471-2597427

*To whom correspondence should be addressed: mahesh@iisertvm.ac.in

Supplementary Information

Experimental Section

Materials. All chemicals were obtained from Sigma Aldrich and used as received without further purification. All reactions were carried out in glassware oven-dried prior to use and wherever necessary, were performed under dry nitrogen in dried, anhydrous solvents using standard gastight syringes, cannulae, and septa. Solvents were dried and distilled by using standard procedures. TLC analyses were performed on precoated aluminum plates of silica gel 60 F254 plates (0.25 mm, Merck) and developed TLC plates were visualized under short- and

long-wavelength UV lamps. Flash column chromatography was performed using silica gel of 200-400 mesh employing a solvent polarity correlated with the TLC mobility observed for the substance of interest. Yields refer to chromatographically and spectroscopically homogenous substances.

Methods. Melting points were obtained using a capillary melting point apparatus and are uncorrected. IR spectra were recorded on a Shimadzu IRPrestige-21 FT-IR spectrometer as neat thin films between NaCl plates in the case of liquids and as KBr pellets in the case of solids. ^{1}H and ^{13}C NMR spectra were measured on a 500 MHz Bruker advanced DPX spectrometer. Internal standard used for ^{1}H and ^{13}C NMR is 1,1,1,1-tetramethyl silane (TMS). All CHN analyses were carried out on an Elementar vario MICRO cube Elemental Analyzer. All values recorded in elemental analyses are given in percentages. Photophysical measurements of **(R/S)-NP(OH)$_2$** gel in DCM/hexane (1:2) mixture were carried out in a cuvette of 1 mm path length unless otherwise mentioned. Absorption and emission spectra were recorded on Shimadzu UV-3600 UV-VIS-NIR and Horiba Jobin Yvon Fluorolog spectrometers respectively. The solid-state fluorescence quantum yield of **(R)-NP(OH)$_2$** in the gel as well as in the thin film state was obtained using an integrating sphere and calculated by Horiba Jobin Yvon quantum yield colour calculator software using tris(8-hydroxyquinolinato)aluminium (Alq$_3$) as standard and is determined to be 0.36 ± 0.04 (Reported quantum yield $\Phi = 0.40$).[1] Circular dichroism spectra was recorded on Jasco J-815 spectrometer. Fluorescence lifetime and anisotropy measurements were carried out in an IBH picosecond time correlated single photon counting (TCSPC) system. Pulse duration (<1 ns and <100 ps) of the excitation peak wavelengths (340 nm and 439 nm) was used as excitation source respectively. Multicomponent decay profile of the dyad **(R)-NP(OH)$_2$** gel resulted in lifetime data that are lower than the pulse duration of the excitation peak wavelength of 340 nm and hence the decay alone is presented in the manuscript (Fig. 2d). The fluorescence decay profiles were de-convoluted using IBH data station software version 2.1, and fitted with exponential decay, minimising the χ^2 values of the fit to 1 ± 0.05. Fluorescence anisotropy decay profiles are corrected for G-factor and r_0 is obtained from a mono-exponential fit of the anisotropy decay. All spectroscopic experiments were performed by using standard quartz cuvettes of path length 1 cm for solution and 1 mm for the gel state in dried and distilled solvents.

Preparation of gel, thin film and solution samples. 1 mM **(R/S)-NP(OH)$_2$** was dissolved in DCM/hexane (1:2) mixture and refrigerated at 0-5 °C for 5-10 minutes. Stability of the gel at ambient temperature was confirmed through the failure of the content to flow on an inverted cuvette. Concentration of **(R/S)-NP(OH)$_2$** in gel state, used for photophysical measurements, is 1 mM (critical gelator concentration) unless otherwise mentioned. The thin film sample was prepared by drop-casting a 1 mM **(R/S)-NP(OH)$_2$** solution in DCM on a fresh clean glass slide and allowed to evaporate the solvent atmospherically in a dust free chamber. 8 μM solution of **(R/S)-NP(OH)$_2$** in DCM is used for solution based photophysical measurements unless otherwise mentioned.

Gelation Studies: Gelation studies were carried out in glass vials of 1 cm diameter. A weighed amount of compound was added to 1 mL of DCM and slowly added to 2 mL of hexane with gentle heating in a water bath. Cooling of the vial in an ice bath provided stable transparent gel. Gel formation was confirmed by the failure of the content to flow on inverting the glass vial. The

critical gelator concentration (CGC) is determined from the minimum amount of gelator required for the formation of a stable gel at room temperature.

X-ray crystallography. Red, single crystals of the dyad (***R***)-NP(OH)$_2$, which exhibited block morphology, was grown from 1 mM gel sample of (***R***)-NP(OH)$_2$ in DCM/hexane (1:2). A high-quality specimen of approximately $0.20 \times 0.15 \times 0.10$ mm^3 was selected for the X-ray diffraction experiment. Crystallographic data collected are presented in the supporting information. Single crystals were mounted using oil (Infineum V8512) on a glass fibre. All measurements were made on a CCD area detector with graphite monochromated Mo Kα radiation. The data was collected using Bruker APEXII detector and processed using APEX2 from Bruker. All structures were solved by direct methods and expanded using Fourier techniques. The non-hydrogen atoms were refined anisotropically. Hydrogen atoms were included in idealized positions, but not refined. Their positions were constrained relative to their parent atom using the appropriate HFIX command in SHELXL-97.

Calculation of radiative decay rate constant.

Radiative (k_r) decay rate constant can be calculated from the following equation[2]

$$k_r = \frac{\Phi_f}{\tau} \qquad (1)$$

where Φ_f is the fluorescence quantum yield and τ is the fluorescence lifetime. In case of multi-exponential decay, weighted average of the fluorescence lifetime values was used to estimate the rate of radiative decay process.

Femtosecond pump-probe transient absorption technique. Spectra-physics Tsunami Oscillator (80 MHz, 780 nm) was used as seed for a Spectra-Physics Spitfire Regenerative amplifier (1 KHz, 4 mJ). A fraction of the amplified output was used to generate 390 nm pump pulse. Residual 780 nm pulse was sent through a delay line inside an ExciPro pump-probe spectrometer from CDP Systems. A rotating CaF$_2$ plate (2 mm thickness) was used to generate continuum of white light from the delayed 780 nm pulses. The continuum of white light was split into two and the streams were used as probe and reference pulses. Transient absorption spectra were recorded using a dual Diode array detector with a 200 nm detection window. Sample solutions were prepared in a rotating sample cell with 400 μm path length. IRF was determined by solvent (10% Benzene in Methanol) two photon absorption and was found to be approximately 130 fs at about 530 nm. Energy per pulse incident on the sample is attenuated employing 80% neutral density filter when required.

The monomeric dyad (***R***)-NP(OH)$_2$ solution (0.75 mM; dichloromethane) in the absence and presence of indole was excited with 390 nm, 1000 nJ, ~100 fs pulses, allowing the selective excitation of naphthalimide unit. At lower concentrations of the dyad (***R***)-NP(OH)$_2$ solution (8 μM) we could not obtain femtosecond transient absorption data having satisfactory signal/noise ratio and hence we increased the concentration of the dyad (***R***)-NP(OH)$_2$ solution (0.75 mM) for FTA measurements. We observed monomeric behavior of the dyad (***R***)-NP(OH)$_2$ in dichloromethane with increase in concentration of (***R***)-NP(OH)$_2$ upto 0.8 mM (Figure S5c,d). The dyad (***R***)-NP(OH)$_2$ thin film was excited with 390 nm, 1000 nJ, ~100 fs pulses for 45

4

minutes to evaluate the photostability of **(R)-NP(OH)$_2$** thin film. In contrast to some of the reported chromophoric systems,[3] our dyad **NP** exhibited identical picosecond fluorescence decay profile (λ_{ex} = 439 nm; λ_{em} = 580 nm; pulse width <100 ps) before and after the laser irradiation (Fig. S20†). Observed high photostability of **(R)-NP(OH)$_2$** thin film could be attributed to a combination of i) rotating sample cell used in our study and ii) exceptional stability of both of the constituents, i.e. naphthalimide and perylenimide units, in the dyad. Vesicular assembly of the dyad **(R)-NP(OH)$_2$** gel in the absence and presence of indole was excited with 390 nm, 200 nJ, ~100 fs pulses, to moderate singlet-singlet annihilation that occurs in multi-chromophoric assemblies.[4] Dyad **(R)-NP(OH)$_2$** gel and dyad **(R)-NP(OH)$_2$**:indole co-gel in the rotating sample cell is mechanically stable throughout the duration of the laser excitation. Kinetic components observed at 597 nm (**PI**$^{\cdot-}$), 620 nm (**^{1}PI***) and 640 (π-π stacked **PI**$^{\cdot-}$) nm are laser intensity independent, ruling out the assignment these kinetic components to singlet−singlet annihilation.[5] Singular value decomposition (SVD) of ΔA versus time and wavelength based three-dimensional map of dyad **(R)-NP(OH)$_2$**:indole co-gel obtained from femtosecond transient absorption (FTA) measurements is demonstrated in Fig. 5c. SVD can estimate the number of independent components contributing to the observed spectral data obtained from the FTA spectral signals. For SVD, the FTA spectra of **(R)-NP(OH)$_2$** containing samples recorded from 520 nm to 680 nm at a timescale of 3.5 ns were constructed into a matrix in the Origin graphics software program (Version 8.5; MicroCal, Inc., Northampton, MA) and subjected to SVD using MATLAB (Version 8.0; The Mathworks, Inc., Natick, MA). The dyad **(R)-NP(OH)$_2$** solution, dyad **(R)-NP(OH)$_2$**+indole (1:10) solution and dyad **(R)-NP(OH)$_2$** gel offered one significant left and right singular vector while the dyad **(R)-NP(OH)$_2$**:indole co-gel offered three significant left singular vectors with significant autocorrelation coefficients. Singular vector observed for the former three cases could be attributed to the **^{1}PI*** centered around 620 nm. While in dyad **(R)-NP(OH)$_2$**:indole co-gel, the three singular vectors yielded corresponds to **PI**$^{\cdot-}$ (597 nm),[6] **^{1}PI*** (620 nm)[7, 8] and π-π stacked **PI**$^{\cdot-}$ (640 nm)[5] respectively. Dyad **(R)-NP(OH)$_2$**:indole (1:500 and 1:1000) solution offered two singular vectors corresponding to **PI**$^{\cdot-}$ (598 nm)[6] and **^{1}PI*** (619 nm)[7, 8] respectively. Global analysis of the FTA spectra of **(R)-NP(OH)$_2$**+indole co-gel/solution were carried out using Glotaran (version 1.2).[9]

Nanosecond transient absorption technique/Laser flash photolysis. Laser flash photolysis experiments of the argon purged solutions were carried out in an Applied Photophysics Model LKS-60 laser kinetic spectrometer using the second and third harmonic (355 nm and 532 nm, pulse duration ≈10 ns) of a Quanta Ray INDI-40-10 series pulsed Nd:YAG laser. Triplet states of the **NI**, **PI** and **(R)-NP(OH)$_2$** in toluene were confirmed using the measurement of oxygen purged solutions through nanosecond flash photolysis studies.

Atomic force microscopy (AFM). Atomic Force Microscopy images were recorded under ambient conditions using multimode scanning probe microscope (Nanoscope V) digital instruments operating in the tapping mode regime. Micro-fabricated silicon cantilever tips (MPP-11100-10) with a resonance frequency of 279–379 KHz and a spring constant of 20–80 Nm^{-1} were used. The scan rate varied from 0.5 Hz to 1.5 Hz. AFM section analysis were done offline. Samples for the imaging were prepared by drop casting dichloromethane (DCM)/hexane (1:2) solution of **(R)-NP(OH)$_2$** on freshly cleaved mica at the required concentrations at ambient conditions. Blank experiments were conducted with solvent alone evaporated on mica to exclude any artefacts. The average diameter of the spherical particles of **(R)-NP(OH)$_2$** was estimated

from the Lorentzian fit of the histogram of the size distribution curves after correcting for the tip-broadening effect.

Transmission electron microscopy (TEM). TEM measurements were carried out using JEOL JEM1011 with an accelerating voltage of 100 kV and the samples were prepared by drop casting DCM/hexane solution of **(R)-NP(OH)₂** onto a carbon-coated copper grid at the required concentrations at ambient conditions and allowing the excess solvent to evaporate atmospherically. TEM images were obtained without staining. The average diameter of the particles was determined from fitted histograms of the size distribution curve.

Scanning electron microscopy (SEM). For SEM measurements, the **(R)-NP(OH)₂** in 1:2 DCM:hexane mixture were drop casted and air dried on the flat surface of cylindrical copper stubs and subjected to thin gold coating using JOEL JFC-1100 fine coater. The probing side was inserted into JEOL JSM-5600 LV scanning electron microscope for obtaining the images. The average diameter of the particles was determined from fitted histograms of the size distribution curve.

Dynamic light scattering (DLS). Dynamic light scattering (DLS) of **(R)-NP(OH)₂** was carried out on a Nano Zeta Sizer, Malvern instruments. The particles were prepared in DCM/hexane solution at the required concentrations at ambient condition.

Optical microscopy. Fluorescent microspheres of **(R)-NP(OH)₂** were observed on a glass slide by using optical microscope (Leica-DMRX Optical Microscope) under the illumination of UV light (365 nm).

X-ray Diffraction (XRD): X-ray diffractograms of the xerogel of **(R)-NP(OH)₂** prepared from 1:2 DCM/hexane solution were recorded on a Philips Diffractometer using Ni filtered Cu Kα radiation.

Determination of Bimolecular Quenching Rate Constant: Biomolecular rate constant (k_q) was estimated from the Stern–Volmer rate constant (K_{sv}) obtained by ploting (τ_0/τ) or (F_0/F) along the Y-axis (where τ_0, τ are the fluorescence lifetimes of **(R)-NP(OH)₂** and F_0 and F are the corresponding fluorescence intensities at the emission maxima in the absence and the presence of the quencher (indole) respectively) and the quencher concentration along the X-axis. The slope of the plot offered K_{sv}. Biomolecular rate constant (k_q) was obtained from the following equation

$$k_q = \frac{K_{SV}}{\tau_0}.$$

Rehm–Weller Analysis: The oxidation potential of indole is found to be 1.1 V[10] and the reduction potentials of **NI** and **PI** are -1.364 and -0.982 V respectively against Saturated Calomel Electrode (SCE). The singlet excited state energies of the acceptor ($E_{0,0}$) values of **NI** and **PI** are found to be 3.65 and 2.56 eV respectively. The change in free energy for the electron transfer (ΔG_{et}) processes were calculated using Rehm–Weller equation, neglecting the Coloumbic interactions to ΔG_{et}.

Synthesis. N-(2,6-diisopropylphenyl)-9-(tributylstannyl))perylene-3,4-dicarboximide (**S1**) was synthesised from 9-bromo-N-(2,6-diisopropylphenyl)-perylene-3,4-dicarboximide following a

previously reported procedure.[11] The dyad **NP(OH)** molecule was synthesised according to previously reported procedure.[12]
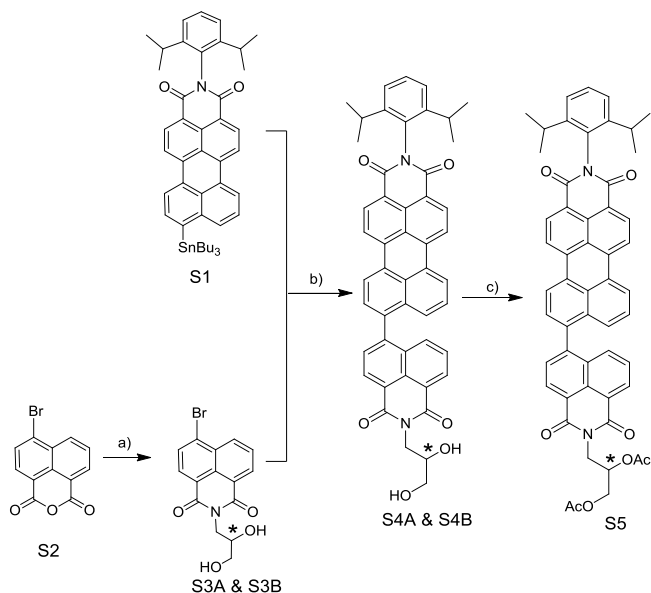
a) 2 3-aminopropanol/H2O;70°C; b) Pd(PPh$_3$)$_4$/DMF/ 90°C; c) acetic anhydride/pyridine/RT.

Scheme S1. Shows the synthesis of (*R/S*)-**NP(OH)$_2$** and the protected analog (*R*)-**NP(OAc)$_2$**.
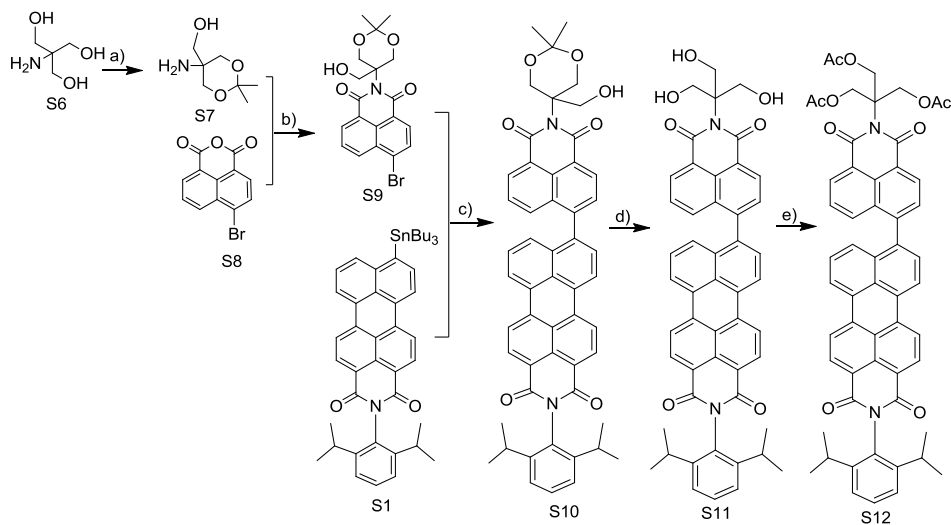
a) Dimethoxy propane/DMF/PTSA; b) pyridine/Zn(OAc)$_2$.2H$_2$O/reflux; c) Pd(PPh$_3$)$_4$ /DMF/ 90°C;
d) MeOH/DCM/1N HCl; e) acetic anhydride/pyridine.

Scheme S2. Shows the synthesis of **NP(OH)$_3$** and the protected analogue **NP(OAc)$_3$**.

Preparation of 4-Bromo-N-((R)-2,3-dihydroxypropyl)-naphthalene-1,8-dicarboximide (S3A) : To a solution of 4-bromo-1,8-naphthalic anhydride **(S2)** (1.00 g, 3.60 mmol) in 100 ml water (R)-3-aminopropane-1,2-diol (1.64 g, 18.00 mmol) was added. This reaction mixture was

heated at 70°C for 5 h following which it was filtered and the precipitate was washed with water and dried. The crude product was then purified by column chromatography (silica gel, EtOAc:petroleum ether 1:1) to afford compound **S3A** (1.13 g, 90%) as a white solid. m. p. 176°C; ^{1}H NMR (500 MHz, CDCl$_3$) δ: 8.71 (d, J = 7.15 Hz, 1H), 8.64 (d, J = 8.45 Hz, 1H), 8.46 (d, J = 7.85 Hz, 1H), 8.09 (d, J = 7.85 Hz, 1H), 7.90 (t, J = 8.15 Hz, 1H), 4.50 − 4.46 (m, 1H), 4.42 − 4.38 (m, 1H), 4.15 − 4.11(m, 1H), 3.72 − 3.64 (m, 2H), 2.13 (s, 2H); ^{13}C NMR (125 MHz, CDCl$_3$) δ: 164.90, 133.96, 132.70, 131.85, 131.30, 131.11, 130.71, 129.05, 128.25, 122.52, 121.62, 70.62, 63.75, 42.79; IR (KBr): 3525, 3379, 3319, 2953, 2873, 1701, 1666, 1587, 1568, 1500, 1458, 1433, 1377, 1336, 1232, 1209, 1101, 1056, 1037, 869, 842, 781, 752 cm^{-1}; Anal. Calcd. for C$_{15}$H$_{12}$BrNO$_4$: C, 51.45; H, 3.45; N, 4.00%. Found: C, 51.51; H, 3.36; N, 3.60%.

Preparation of 4-Bromo-N-((S)-2,3-dihydroxypropyl)-naphthalene-1,8-dicarboximide (S3B) : To a solution of 4-bromo-1,8-naphthalic anhydride **(S2)** (1.00 g, 3.60 mmol) in 100 ml water (R)-3-aminopropane-1,2-diol (1.64 g, 18.00 mmol) was added. This reaction mixture was heated at 70°C for 5 h following which it was filtered and the precipitate was washed with water and dried. The crude product was then purified by column chromatography (silica gel, EtOAc:petroleum ether 1:1) to afford compound **S3B** (1.13 g, 90%) as a white solid. m. p. 176°C; ^{1}H NMR (500 MHz, CDCl$_3$) δ: 8.60 (d, J = 7.25 Hz, 1H), 8.53 (d, J = 8.15 Hz, 1H), 8.36 (d, J = 7.85 Hz, 1H), 7.99 (d, J = 7.85 Hz, 1H), 7.79 (t, J = 8.15 Hz, 1H), 4.39 − 4.35 (m, 1H), 4.31 − 4.28 (m, 1H), 4.04 − 4.00 (m, 1H), 3.61 − 3.53 (m, 2H), 2.09 (s, 2H); ^{13}C NMR (125 MHz, CDCl$_3$) δ: 164.86, 133.91, 132.66, 131.81, 131.29, 131.05, 130.73, 129.07, 128.23, 122.57, 121.67, 70.68, 63.82, 42.84; IR (KBr): 3527, 3383, 2954, 1701, 1668, 1587, 1570, 1500, 1458, 1433, 1377, 1336, 1234, 1209, 1103, 1056, 1037, 869, 842, 781, 752 cm^{-1}; Anal. Calcd. for C$_{15}$H$_{12}$BrNO$_4$: C, 51.45; H, 3.45; N, 4.00%. Found: C, 51.61; H, 3.62; N, 4.25%.

Preparation of 9-(4-(N-(R)-2,3-dihydroxypropyl)naphthalene-1,8-dicarboximide)yl)-N-(2,6-diisopropylphenyl)-perylene-3,4-dicarboximide (S4A) : A solution of N-(2,6-diisopropylphenyl)-9-(tributylstannyl))perylene-3,4-dicarboximide **(S1)** (0.686 g, 0.89 mmol), 4-Bromo-N-((R)-2,3-dihydroxypropyl)-naphthalene-1,8-dicarboximide **(S3A)** (0.61 g, 1.12 mmol) and Pd(PPh$_3$)$_4$ (10.28 mg, 0.0089 mmol) in 50 ml DMF was heated at 90 °C for 2 days. The solvent was removed under reduced pressure and the residue was purified by column chromatography (silica gel, EtOAc:petroleum ether 1:1) to afford compound **S4A** (0.46 g, 70%) as a yellow-orange solid. m. p. > 300°C; ^{1}H NMR (500 MHz, CDCl$_3$,) δ: 8.73 (d, J = 7.40 Hz, 1H), 8.67 − 8.63 (m, 3H), 8.57 (d, J = 7.85 Hz, 1H), 8.52 (d, J = 8.15 Hz, 1H), 8.47 (d, J = 8.0 Hz, 2H), 7.87 (d, J = 8.45 Hz, 1H), 7.82 (d, J = 7.40 Hz, 1H), 7.62 − 7.58 (m, 2H), 7.47 − 7.40 (m, 2H), 7.34 (d, J = 8.35 Hz, 1H), 7.28 (d, J = 7.8 Hz, 2H), 4.48 − 4.45 (m, 1H), 4.42 − 4.38 (m, 1H), 4.11 − 4.09 (m, 1H), 3.64 − 3.62 (m, 2H), 2.73 − 2.69 (m, 2H), 2.20 (s, 2H), 1.13 − 1.11 (m, 12H); ^{13}C NMR (125 MHz, CDCl$_3$) δ: 164.43, 164.27, 162.89, 144.71, 144.68, 144.06, 137.82, 136.20, 135.91, 132.37, 132.20, 131.16, 131.11, 130.42, 130.15, 129.92, 129.51, 129.51, 129.16, 128.77 128.49, 128.13, 128.09, 127.75, 127.58, 127.28, 126.71, 126.44, 125.99, 123.10, 123.03, 122.08, 121.45, 121.14, 120.59, 120.44, 119.80, 69.76, 62.76, 41.78, 28.16, 23.01, 23.00; IR (KBr): 3549, 3442, 2958, 2866, 1697, 1654, 1591, 1577, 1359, 1234, 1180, 1083, 1031, 812, 788, 758 cm^{-1}; Anal. Calcd. for C$_{49}$H$_{38}$N$_2$O$_6$: C, 78.38; H, 5.10; N, 3.73%. Found: C, 78.25; H, 5.27; N, 3.06%.

Preparation of 9-(4-(N-(S)-2,3-hydroxypropyl)naphthalene-1,8-dicarboximide)yl)-N-(2,6-diisopropylphenyl)-perylene-3,4-dicarboximide (S4B) : A solution of N-(2,6-diisopropylphenyl)-9-(tributylstannyl))perylene-3,4-dicarboximide (**S1**) (0.686 g, 0.89 mmol), 4-Bromo-N-((S)-2,3-dihydroxypropyl)-naphthalene-1,8-dicarboximide **(S3B)** (0.61 g, 1.12 mmol) and Pd(PPh$_3$)$_4$ (10.28 mg, 0.0089 mmol) in 50 ml DMF was heated at 90°C for 2 days. The solvent was removed under reduced pressure and the residue was purified by column chromatography (silica gel, EtOAc:petroleum ether 1:1) to afford compound **S4B** (0.43 g, 65%) as a red-orange solid. m. p. > 300°C; ^{1}H NMR (500 MHz, CDCl$_3$) δ: 8.82 (d, J = 7.40 Hz, 1H), 8.76 − 8.72 (m, 3H), 8.66 (d, J = 7.80 Hz, 1H), 8.60 (d, J = 8.15 Hz, 1H), 8.55 (d, J = 8.05 Hz, 2H), 7.97 (d, J = 8.45 Hz, 1H), 7.92 (d, 7.40 Hz, 1H), 7.73 − 7.68 (m, 2H), 7.57 − 7.50 (m, 2H), 7.44 (d, J = 8.35 Hz, 1H), 7.38 (d, J = 7.80 Hz, 2H), 4.58 − 4.54 (m, 1H), 4.50 − 4.47 (m, 1H), 4.22 − 4.18 (m, 1H), 3.77 − 3.70 (m, 2H), 2.84 − 2.79 (m, 2H), 2.36 (s, 2H), 1.23 − 1.21 (m, 12H); ^{13}C NMR (125 MHz, CDCl$_3$) δ: 165.46, 165.26, 163.94, 145.74, 145.71, 145.06, 138.87, 137.25, 136.95, 133.38, 133.22, 132.19, 132.15, 131.44, 131.17, 130.93, 130.52, 130.14, 129.75, 129.54, 129.17, 129.12, 128.81, 128.59, 128.28, 127.74, 127.48, 126.98, 124.16, 124.07, 123.14, 122.47, 122.16, 121.56, 121.40, 120.82, 120.70, 70.75, 63.83, 42.80, 31.60, 29.19, 24.05, 24.03; IR (KBr): 3549, 3442, 2958, 2868, 1697, 1654, 1591, 1506, 1359, 1296, 1242, 1180, 1085, 1031, 921, 844, 812, cm^{-1}; Anal. Calcd. for C$_{49}$H$_{38}$N$_2$O$_6$: C, 78.38; H, 5.10; N, 3.73%. Found: C, 78.51; H, 5.25; N, 3.89%.

Preparation of 9-(4-(N-(R)-2,3-diacetoxypropyl)naphthalene-1,8-dicarboximide)yl)-N-(2,6-diisopropylphenyl)-perylene-3,4-dicarboximide (S5) : A solution of 9-(4-(N-(R)-2,3-dihydroxypropyl)naphthalene-1,8-dicarboximide)yl)-N-(2,6-diisopropylphenyl)-perylene-3,4-dicarboximide **(S4A)** (0.100 g, 0.13 mmol), acetic anhydride (0.136 g, 1.3 mmol) in 5 ml pyridine were stirred at room temperature for 12 h. The solvent was removed under reduced pressure and the residue was purified by column chromatography (silica gel, EtOAc:petroleum ether 1:2) to afford compound **S5** (0.11 g, 95%) as a yellow-orange solid. m. p. > 300°C; ^{1}H NMR (500 MHz, CDCl$_3$) δ: 8.69 (d, J = 7.40 Hz, 1H), 8.66 − 8.63 (m, 2H), 8.59 − 8.56 (m, 2H), 8.51 (d, J = 8.15 Hz, 1H), 8.46 (d, J = 7.95 Hz, 2H), 7.84 − 7.82 (m, 1H), 7.78 (d, J = 7.40 Hz, 1H), 7.61 (d, J = 7.65 Hz, 1H), 7.57 (d, J = 7.8 Hz, 1H), 7.48 − 7.36 (m, 3H), 7.28 (d, J = 7.8 Hz, 2H), 5.53 − 5.51 (m, 1H), 4.62 − 4.59 (m, 1H), 4.38 − 4.34 (m, 2H), 4.26 − 4.23 (m, 1H), 2.73 − 2.69 (m, 2H), 2.06 (s, 3H), 1.97 (s, 3H), 1.13 − 1.11 (m, 12H); ^{13}C NMR (125 MHz, CDCl$_3$) δ : 170.71, 164.28, 164.12, 163.94, 145.75, 145.72, 144.66, 139.09, 137.30, 137.02, 133.42, 132.87, 132.19, 132.15, 131.81, 131.23, 130.96, 130.55, 130.07, 129.73, 129.52, 129.14, 129.00, 128.64, 128.28, 127.71, 127.36, 127.02, 124.15, 124.06, 123.16, 122.66, 122.37, 121.55, 121.40, 120.79, 120.66, 69.83, 63.74, 40.65, 29.18, 24.05, 24.03, 20.98, 20.83; IR (KBr): 2958, 2960, 2868, 1743, 1701, 1622, 1587, 1357, 1238, 1045, 812, 788, 758 cm^{-1}; Anal. Calcd. for C$_{53}$H$_{42}$N$_2$O$_8$: C, 76.24; H, 5.07; N, 3.36%. Found: C, 76.35; H, 5.27; N, 3.06%.

Preparation of (5-amino-2,2-dimethyl-1,3-dioxan-5-yl) methanol (S7) : A solution of 2-Amino-2-hydroxymethyl-propane-1,3-diol **(S6)** (5.00 g, 0.032 mmol) and p-toluene sulfonic acid (0.0297 g, 0.0016 mmol) in 50 ml DMF were stirred overnight. To this 0.4 ml triethyl amine (TEA) was added and solvent evaporated under reduced pressure. The residue is then

precipitated by methanol and filtered. To the filterate 2.5 ml TEA added again filtered . The filtrate is then concentrated and purified by column chromatography (silica gel, EtOAc:methanol 9:1) to afford compound **S7** (2.56 g, 50%) as a white solid. m. p. 32°C; ^{1}H NMR (500 MHz, CDCl$_3$) δ: 3.80 (d, J = 11.5 Hz, 2H), 3.58 (d, J = 11.5 Hz, 2H), 3.52 (s, 2H), 1.45 (s, 3H), 1.42 (s, 3H); ^{13}C NMR (125 MHz, CDCl$_3$) δ: 98. 52, 66.71, 64.30, 50.67, 25.20, 21.87; IR (KBr): 3323, 3269, 2954, 2864, 1612, 1479, 1458, 1369, 1294, 1247, 1199, 1155, 1101, 1051, 1004, 933, 827 cm^{-1}; Anal. Calcd. for C$_7$H$_{15}$NO$_3$: C, 52.16; H, 9.38; N, 8.69%. Found: C, 52.51; H, 9.56; N, 8.90%.

Preparation of 4-Bromo-N-(5(2-hydroxymethyl 2,2-dimethyl-1,3-dioxan)-naphthalene-1,8-dicarboximide (S9) : To a solution of 4-bromo-1,8-naphthalic anhydride **(S8)** (2.00 g, 7.20 mmol), (5-amino-2,2-dimethyl-1,3-dioxan-5-yl) methanol **(S7)** (1.74 g, 10.83 mmol), zinc acetate (0.946 g, 4.32 mmol) in 10 ml pyridine was added. This reaction mixture was refluxed overnight. The solvent was removed under reduced pressure and the residue purified by column chromatography (silica gel, EtOAc:petroleum ether 1:1) to afford compound **S9** (0.605 g, 20%) as a white solid. m. p. 186°C; ^{1}H NMR (500 MHz, CDCl$_3$) δ: 8.45 – 8.43 (m, 2H), 8.22 (d, J = 7.85 Hz, 1H), 7.93 (d, J = 7.85 Hz, 1H), 7.75 (t, J = 7.90 Hz, 1H), 4.41 (d, J = 12.85, 2H), 4.30 (d, J = 12.85, 2H), 4.23 (s, 2H), 1.30 (s, 3H), 1.24 (s, 3H); ^{13}C NMR (125 MHz, CDCl$_3$) δ: 166.14, 166.09, 133.06, 131.81, 131.15, 131.03, 130.29, 130.02, 128.65, 128.19, 124.39, 123.49, 99.84, 68.01, 64.45, 62.86, 23.49, 23.30; IR (KBr): 3437, 2947, 2899, 1705, 1660, 1579, 1346, 1232, 1074, 1035, 840, 781 cm^{-1}; Anal. Calcd. for C$_{19}$H$_{18}$BrNO$_5$: C, 54.30; H, 4.32; N, 3.33%. Found: C, 54.61; H, 4.36; N, 3.60%.

Preparation of 9-(4-(N-(5(2-hydroxymethyl 2,2-dimethyl-1,3-dioxan)-naphthalene-1,8-dicarboximide)yl)-N-(2,6-diisopropylphenyl)-perylene-3,4-dicarboximide (S10) : A solution of N-(2,6-diisopropylphenyl)-9-(tributylstannyl))perylene-3,4-dicarboximide **(S1)** (0.686 g, 0.89 mmol), 4-Bromo-N-(5(2-hydroxymethyl 2,2-dimethyl-1,3-dioxan)-naphthalene-1,8-dicarboximide (**S9**) (0.61 g, 1.12 mmol) and Pd(PPh$_3$)$_4$ (10.28 mg, 0.0089 mmol) in 50 ml DMF was heated at 90°C for 2 days. The solvent was removed under reduced pressure and the residue was purified by column chromatography (silica gel, EtOAc:petroleum ether 1:1) to afford compound **S10** (0.46 g, 70%) as a yellow-orange solid. m. p. > 300°C; ^{1}H NMR (500 MHz, CDCl$_3$) δ: 8.66 – 8.63 (m, 2H), 8.60 (d, J = 7.35 Hz, 1H), 8.56 (d, J = 7.80 Hz, 1H), 8.52 – 8.45 (m, 4H), 7.81 – 7.77 (m, 2H), 7.61 (7.65 Hz, d, 1H), 7.58 – 7.55 (m, 1H), 7.47 – 7.40 (m, 2H), 7.34 (d, J = 8.4, 1H), 7.28 (d, J = 7.75 Hz, 2H), 4.48 (d, J = 12.9 Hz, 2H), 4.37 (d, J = 13.00 Hz, 2H), 4.30 (s, 2H), 2.74 – 2.68 (m, 2H), 1.34 (s, 3H), 1.30 (s, 3H) 1.13 – 1.11 (m, 12H); ^{13}C NMR (125 MHz, CDCl$_3$) δ: 166.74, 166.57, 163.94, 145.73, 145.70, 144.20, 139.00, 133.39, 132.40, 132.19, 132.15, 131.33, 130.95, 130.81, 130.59, 130.54, 130.08, 129.75, 129.53, 129.16, 129.04, 128.86 128.29, 127.70, 127.46, 127.01, 124.40, 124.14, 124.11, 124.07, 123.16, 121.54, 121.41, 120.79, 120.67, 99.92, 68.07, 64.78, 62.97, 29.97, 24.06, 24.04, 23.45, 23.42; IR (KBr): 3498, 2947, 2899, 1705, 1660, 1579, 1346, 1232, 1074, 1035, 840, 781 cm^{-1}; Anal. Calcd. for C$_{53}$H$_{44}$N$_2$O$_7$: C, 77.54; H, 5.40; N, 3.41%. Found: C, 77.25; H, 5.27; N, 3.06%.

Preparation of 9-(4-(N-(2(2-hydroxymethyl 1,3-dihydroxypropyl)naphthalene-1,8-dicarboximide)yl)-N-(2,6-diisopropylphenyl)-perylene-3,4-dicarboximide (S11) : A solution of 9-(4-(N-(5(2-hydroxymethyl 2,2-dimethyl-1,3-dioxan)-naphthalene-1,8-dicarboximide)yl)-N-(2,6-diisopropylphenyl)-perylene-3,4-dicarboximide **(S10)** (0.200 g, 0.24 mmol), 1N HCl (0.24

ml, 0.24 mmol) in 5 ml dichloromethane and 5 ml methanol were stirred at room temperature for 1 hour. The solvent was removed under reduced pressure and the residue was purified by column chromatography (silica gel, EtOAc:petroleum ether 2:1) to afford compound **S11** (0.17 g, 90%) as a yellow-orange solid. m. p. > 300°C; ; ^{1}H NMR (500 MHz, DMSO-d$_6$, 373 K) δ: 8.89 – 8.76 (m, 4H), 8.63 (t, J = 8.5 Hz, 2H), 8.49 (d, J = 7.5 Hz, 1H), 7.87 – 7.75 (m, 3 H), 7.67 – 7.52 (m, 2H), 7.50 – 7.43 9 (m, 2H), 7.36 (d, J = 7.5 Hz, 2H),7.21 – 7.14 (m, 1H), 5.58 (s, 1H), 4.71 (s, 1H), 4.43 (d, J = 8.5 Hz, 2H), 4.30 (s, 1H), 4.18 (d, J = 11 Hz, 1H), 4.02 (d, 10.5 Hz, 1H), 3.95 (d, 13 Hz, 2H), 2.79 – 2.73 (m, 2H), 1.15 – 1.13 (m, 12H); IR (KBr): 3431, 2960, 2868, 1699, 1654, 1589, 1573, 1357, 1246, 1031, 840, 781 cm^{-1}; Anal. Calcd. for $C_{50}H_{40}N_2O_7$: C, 76.91; H, 5.16; N, 3.59%. Found: C, 76.25; H, 5.57; N, 3.16%. HRMS–TOF–MS Calcd. for [M+H]$^+$ 781.8697; found 781.2737.

Preparation of 9-(4-(N-(2(2-acetoxoxymethyl 1,3-aetoxypropyl)naphthalene-1,8-dicarboximide))-perylene-3,4-dicarboximide (S12) :

A solution of 9-(4-(N-(2(2-hydroxymethyl 1,3-dihydroxypropyl)naphthalene-1,8-dicarboximide)yl)-N-(2,6-diisopropylphenyl)-perylene-3,4-dicarboximide **(S11)** (0.05 g, 0.06 mmol), acetic anhydride (0.98 g, 0.96 mmol in 5 ml pyridine were stirred at room temperature for 12 hours. The solvent was removed under reduced pressure and the residue was purified by column chromatography (silica gel, EtOAc:petroleum ether 1:3) to afford compound **S12** (0.055 g, 95%) as a yellow-orange solid. m. p. > 300°C; ^{1}H NMR (500 MHz, CDCl$_3$) δ: 8.66 – 8.59 (m, 3H), 8.56 (d, J = 8.00 Hz, 1H), 8.49 – 8.45 (m, 4H), 7.81 – 7.77 (m, 2H), 7.61 – 7.55 (m, 2H), 7.47 – 7.38 (m, 3H), 7.28 (d, J = 8.00 Hz, 2H), 4.98 (s, 6H), 2.72 – 2.70 (m, 2H), 1.97 (s, 9H), 1.13 – 1.11 (m, 12H); ^{13}C NMR (125 MHz, CDCl$_3$) δ: 170.32, 166.02, 165.86, 163.91, 163.89, 145.77, 145.74, 143.99, 139.04, 137.26, 136.98, 133.41, 132.14, 132.10, 131.26, 131.00, 130.83, 130.53, 130.10, 129.79, 129.49, 129.14, 129.07, 128.87 128.33, 128.17, 127.66, 127.44, 127.02, 124.48, 124.15, 124.11, 124.03, 123.12, 121.61, 121.48, 120.79, 120.66, 67.07, 62.66, 29.19, 24.02, 24.00, 20.79; IR (KBr): 2964, 2870, 1747, 1703, 1664, 1587, 1359, 1224, 1043, 1035, 840, 781 cm^{-1}; Anal. Calcd. for $C_{56}H_{46}N_2O_{10}$: C, 74.16; H, 5.16; N, 3.59%. Found: C, 74.25; H, 5.27; N, 3.06%.

References
1. M. Cölle, J. Gmeiner, W. Milius, H. Hillebrecht and W. Brütting, *Adv. Funct. Mater.*, 2003, **13**, 108-112.
2. J. R. Lakowicz, *Principles of Fluorescence Spectroscopy*, Springer, New York, 2006.
3. R. J. Dillon and C. J. Bardeen, *J. Phys. Chem. A*, 2011, **115**, 1627-1633.
4. J. Larsen, B. Brüggemann, T. Polívka, V. Sundström, E. Åkesson, J. Sly and M. J. Crossley, *J. Phys. Chem. A*, 2005, **109**, 10654-10662.
5. K. M. Lefler, D. T. Co and M. R. Wasielewski, *J. Phys. Chem. Lett.*, 2012, **3**, 3798-3805.
6. D. Gosztola, M. P. Niemczyk, W. Svec, A. S. Lukas and M. R. Wasielewski, *J. Phys. Chem. A*, 2000, **104**, 6545-6551.
7. F. Odobel, M. Séverac, Y. Pellegrin, E. Blart, C. Fosse, C. Cannizzo, C. R. Mayer, K. J. Elliott and A. Harriman, *Chem.–Eur. J.*, 2009, **15**, 3130-3138.
8. T. D. M. Bell, A. Stefan, S. Masuo, T. Vosch, M. Lor, M. Cotlet, J. Hofkens, S. Bernhardt, K. Müllen, M. van der Auweraer, J. W. Verhoeven and F. C. De Schryver, *ChemPhysChem*, 2005, **6**, 942-948.
9. J. J. Snellenburg, S. P. Laptenok, R. Seger, K. M. Mullen and I. H. M. van Stokkum, *J. Stat. Soft.*, 2012, **49**, 1–22.
10. J. Pérez-Prieto, F. Boscá, R. E. Galian, A. Lahoz, L. R. Domingo and M. A. Miranda, *J. Org. Chem.*, 2003, **68**, 5104-5113.
11. F. O. Holtrup, G. R. J. Müller, H. Quante, S. De Feyter, F. C. De Schryver and K. Müllen, *Chem.–Eur. J.*, 1997, **3**, 219-225.
12. R. T. Cheriya, J. Joy, A. P. Alex, A. Shaji and M. Hariharan, *J. Phys. Chem. C*, 2012, **116**, 12489-12498.

Table S1. Single crystal X-ray and structure refinement data for the dyad **(R)-NP(OH)₂**.

Emperical fomula	$C_{49}H_{38}O_6N_2$
Fomula weight	750.81
Temperature	296(2) K
Wavelength	0.71073 Å
Crystal system	Triclinic
Space group	*P*-1
Unit cell dimensions	a = 8.947 Å $\quad$ α = 75.26°
	b = 14.538 Å $\quad$ β = 78.85°
	c = 14.887 Å $\quad$ γ = 82.01°
Volume	1829.1 Å³
Z, Calculated density	2, 1.363 Mg/m³
Absorption coefficient	0.090 mm⁻¹
F(000)	788
Crystal size	0.20 x 0.15 x 0.10 mm³
Theta range for data collection	1.43 to 25.00°
Index ranges	-10<=h<=10, -17<=k<=17, -17<=l<=17
Reflections collected	23878
Independent Reflections	6369 [R(int) = 0.0966]
Completeness to theta = 25.00°	98.5 %
Absorption correction	Semi-empirical from equivalents
Refinement method	Full-matrix least-squares on F^2
Data / restraints / parameters	6369 / 5 / 509
Goodness-of-fit on F^2	1.521
Final R indices [I>2sigma(I)]	R1 = 0.1541, wR2 = 0.4212
R indices (all data)	R1 = 0.2678, wR2 = 0.5014
Extinction coefficient	0.007(5)
Largest diff. peak and hole	1.102 and -1.044 e. Å⁻³

Table S2. Gel stability of vesicular **(R)-NP(OH)₂** in the presence and absence of indole. Critical gelator concentration [a](CGC) of **(R)-NP(OH)₂** in DCM:hexane (1:2) in the absence and presence of indole.

Gel Sample	CGC (mg/mL)
NP(OH)₂	0.75
NP(OH)₂ + Indole (1: 6.7)	0.75
NP(OH)₂ + Indole (1: 13.3)	0.75
NP(OH)₂ + Indole (1: 26.6)	0.75
NP(OH)₂ + Indole (1: 66.6)	0.75
NP(OH)₂ + Indole (1: 100)	0.75

[a]CGC is the minimum concentration of the gelator required for the formation of a stable gel at room temperature.

Table S3. Shows the rate of fluorescence decay (k_f) and rate of charge recombination (k_{cr}) in the dyad (**R**)-**NP(OH)₂** under different conditions upon photoexcitation

| Context	τ_f (ns)[a]	k_f ($\times 10^8$ s⁻¹)	$k_q[M]$[b] ($\times 10^8$ s⁻¹)	$\tau_{1_{PI^*}}$ (ns)[c]	τ_{cr}[d]	k_{cr} (s⁻¹)
NP(OH)₂ solution	3.7	$k_{f1} = 2.7$	-	3.0	≤ 110 fs	$k_{cr1} \leq 9.0 \times 10^{12}$
NP(OH)₂:indole (1:1000) solution	3.3	$k_{f2} = 3.0$	0.5	0.5	6.5 ps	$k_{cr2} = 1.5 \times 10^{11}$
NP(OH)₂:indole (1:500) solution	3.5	$k_{f2'} = 2.8$	0.25	0.64	6.0 ps	$k_{cr2'} = 1.7 \times 10^{11}$
NP(OH)₂:indole (1:10) solution	3.7	$k_{f2''} = 2.7$	0.005	2.9	≤ 110 fs	$k_{cr2''} \leq 9.0 \times 10^{12}$
NP(OH)₂ gel	3.8	$k_{f3} = 2.6$	-	2.9	≤ 110 fs	$k_{cr3} \leq 9.0 \times 10^{12}$
NP(OH)₂:indole (1:10) co-gel	2.4	$k_{f4} = 4.2$	0.7	3.0	2.1 ps / 1.4 ns	$k_{cr4} = 4.8 \times 10^{11}$ / $k_{cr4'} = 7.4 \times 10^{8}$

[a] obtained from TCSPC measurements when excited at 340 nm using 8 μM (**R**)-**NP(OH)₂** [b] [M] stands for the molar concentration of indole [c] obtained from FTA measurements using 0.75 mM (**R**)-**NP(OH)₂** [d] excited at 390 nm
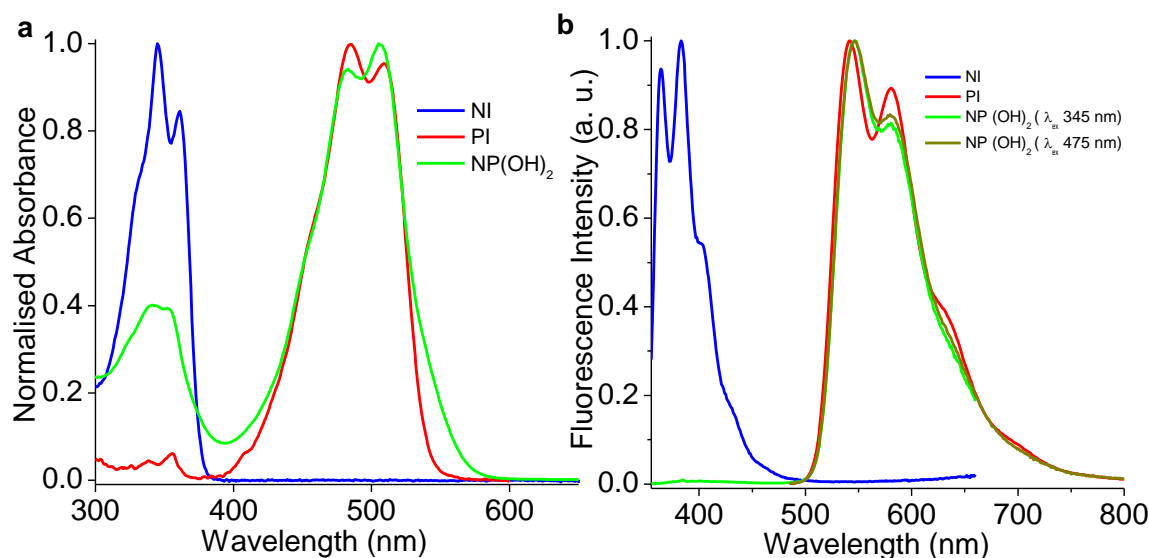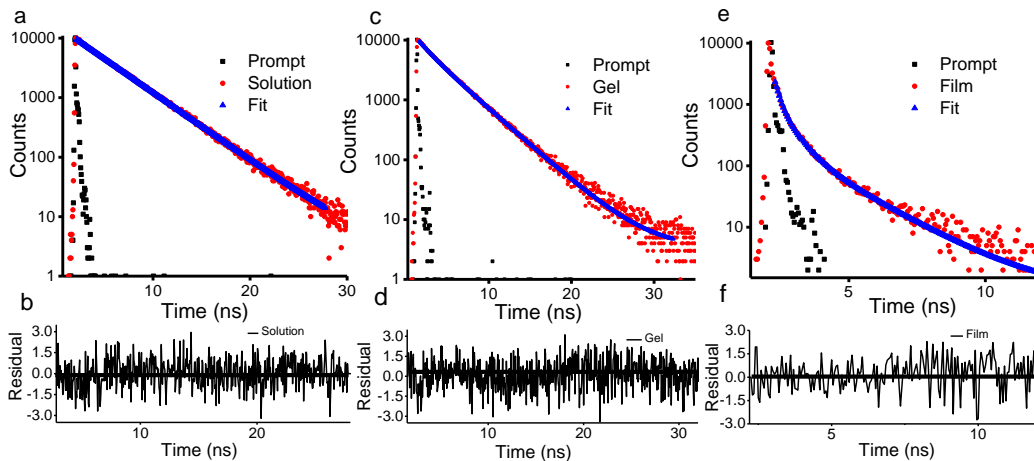

Figure S1. Absorption and fluorescence emission properties. (a) Absorption spectra of **NI** (blue), **PI** (red) and (**R**)-**NP(OH)₂** (green) in DCM and (b) Fluorescence emission spectra of **NI** (blue; λ_{ex}: 345 nm), **PI** (red; λ_{ex}: 475 nm) and (**R**)-**NP-(OH)₂** (green; λ_{ex}: 345 nm and dark yellow; λ_{ex}: 475 nm) in DCM.
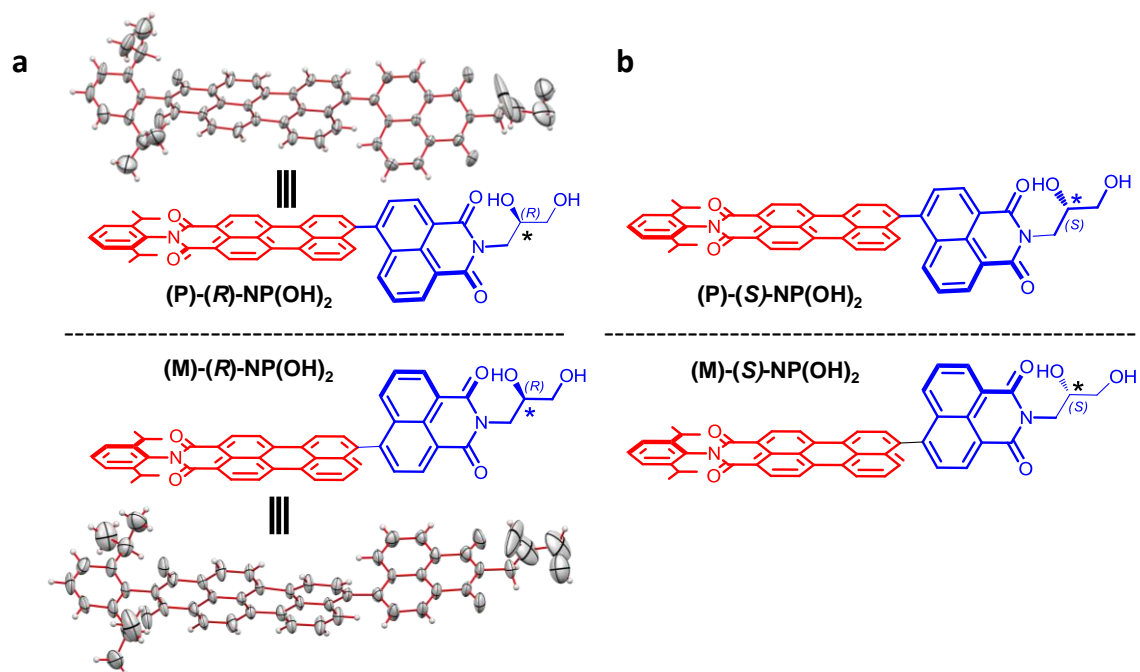
Figure S2. Chemical structure of two optical isomers of **(P/M)-NP(OH)₂**. The molecular structure of the P and M stereoisomers of (a) **(R)-NP(OH)₂** and (b) **(S)-NP(OH)₂**. (a) X-ray structure of the P and M stereoisomers of **(R)-NP(OH)₂** are also shown.
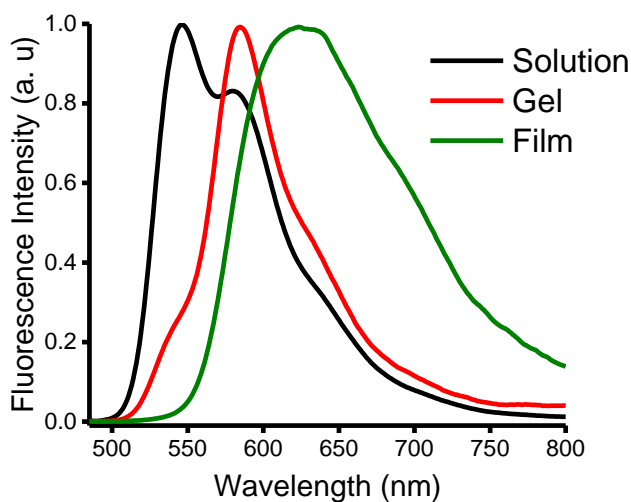

Figure S3. Fluorescence emission spectra of **(R)-NP(OH)₂** in solution, gel and film. Fluorescence emission spectra of **(R)-NP(OH)₂** in DCM [black], **(R)-NP(OH)₂** gel in DCM:hexane (1:2) mixture [red], **(R)-NP(OH)₂** thin film [green] when excited at 475 nm.

Figure S4. Fluorescence decay profile of **(R)-NP(OH)$_2$** in solution (8 μM), gel (1 mM) and film (1 mM). Time-resolved fluorescence decay of **(R)-NP(OH)$_2$** in (a) DCM solution; (b) corresponding residual fit; (c) gel; (d) corresponding residual fit; (e) thin film and (f) corresponding residual fit when excited at 439 nm and monitored at 550 nm (solution) and 580 nm (gel and film).
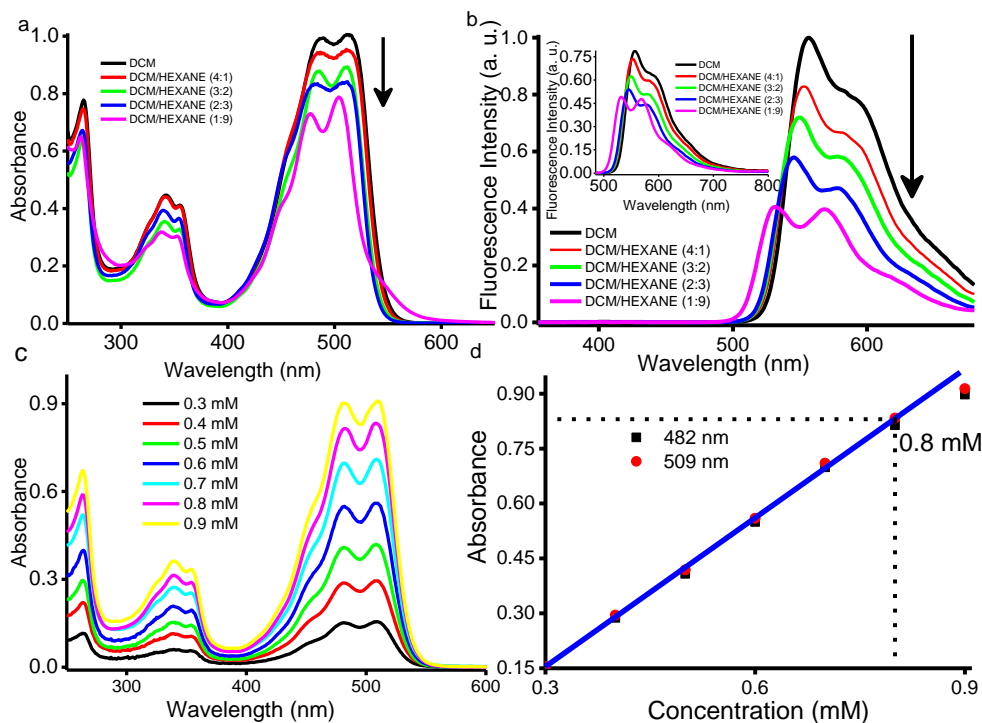
Figure S5. Aggregation dependent change in absorption and fluorescence spectra. (a) Absorption spectra of **(R)-NP(OH)$_2$** (8 μM) in DCM with increasing concentration of hexane and (b) Fluorescence emission spectra **(R)-NP(OH)$_2$** in DCM with increasing concentration of hexane (λ$_{ex}$: 345 nm); inset shows the corresponding emission spectra (λ$_{ex}$: 475 nm); (c) concentration dependent absorption spectra of **(R)-NP(OH)$_2$** in DCM and (d) variation of absorbance at the two λ$_{max}$ (482 and 509 nm) with concentration of **(R)-NP(OH)$_2$** in DCM .
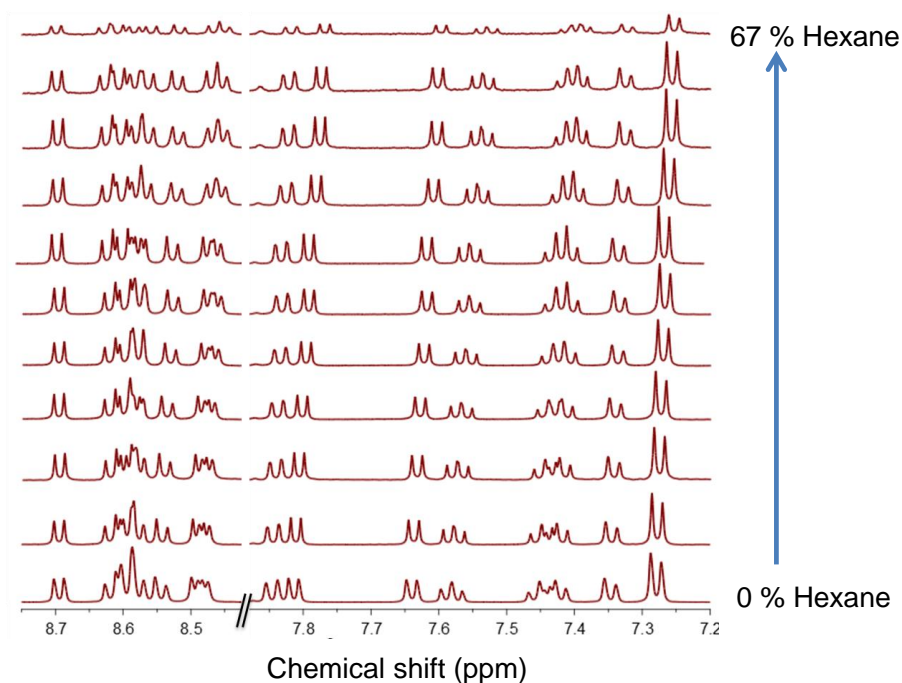
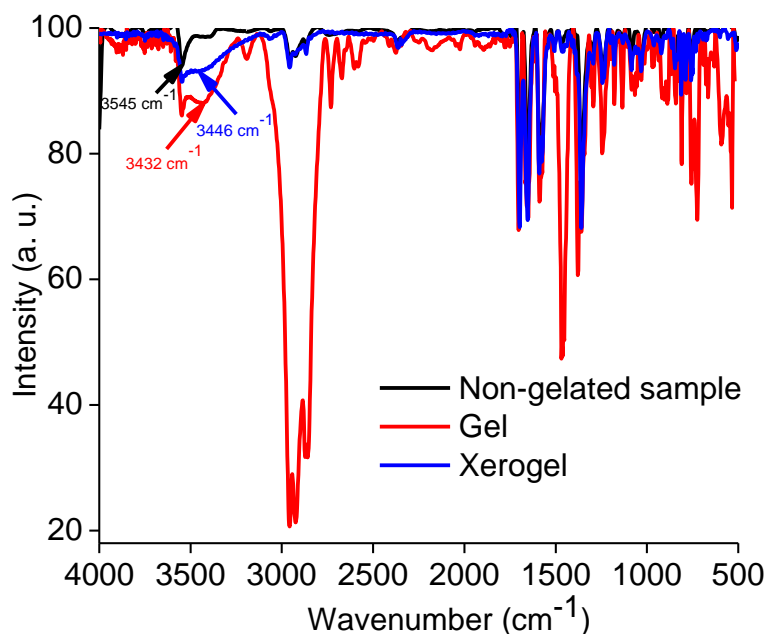**Figure S6.** ^{1}HNMR investigation of intermolecular aggregation. ^{1}HNMR titration of 13.3 mM **(R)-NP(OH)$_2$** in CD_2Cl_2 with increasing concentration of hexane.
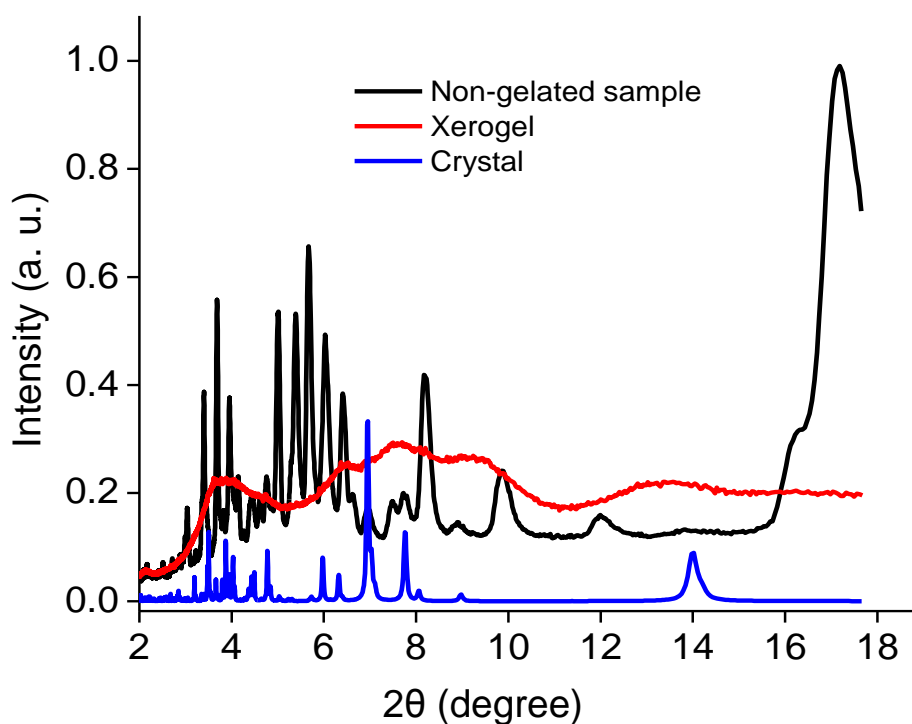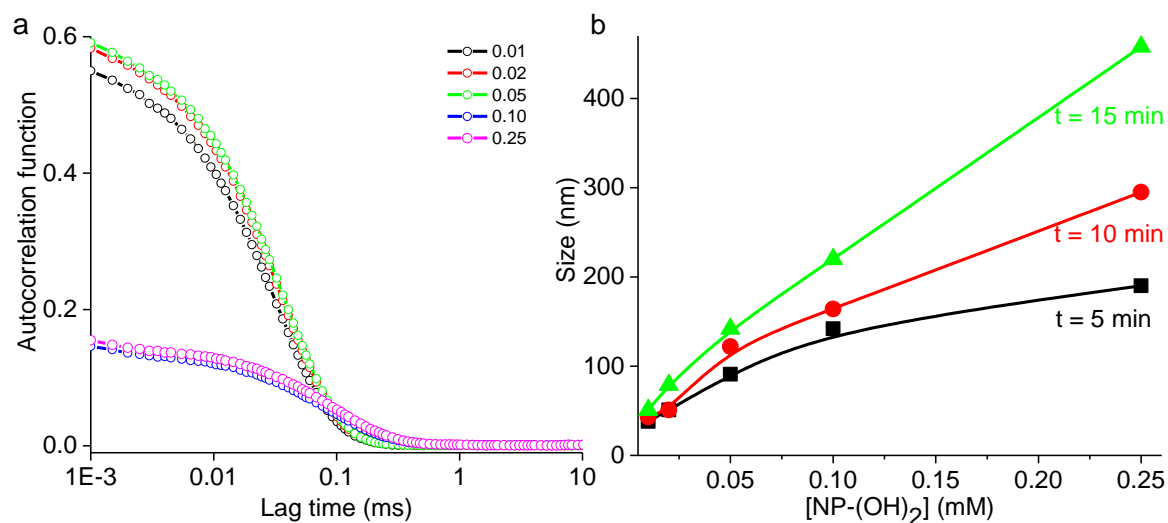

Figure S7. X-ray powder diffracton. Powder X-ray diffraction patterns of **(R)-NP(OH)$_2$** xerogel (red), non-gelated (black) and crystalline sample (blue).

Figure S8. FTIR characterisation. Infrared absorption spectra of **(R)-NP(OH)$_2$** in non gelated (black), gel (red) and xerogel sample (blue).


Figure S9. Concentration and time dependent dynamic light scattering. (a) Autocorrelation function of **(R)-NP(OH)$_2$** spherical assemblies in DCM:hexane (1:2) mixture with increasing concentration of **(R)-NP(OH)$_2$** (0.01–0.25 mM) and (b) variation of the hydrodynamic diameter of **(R)-NP(OH)$_2$** spherical assemblies in DCM:hexane (1:2) mixture with increase in time (5–15 min) and concentration of **(R)-NP(OH)$_2$** (0.01–0.25 mM) determined using dynamic light scattering (DLS) measurement.
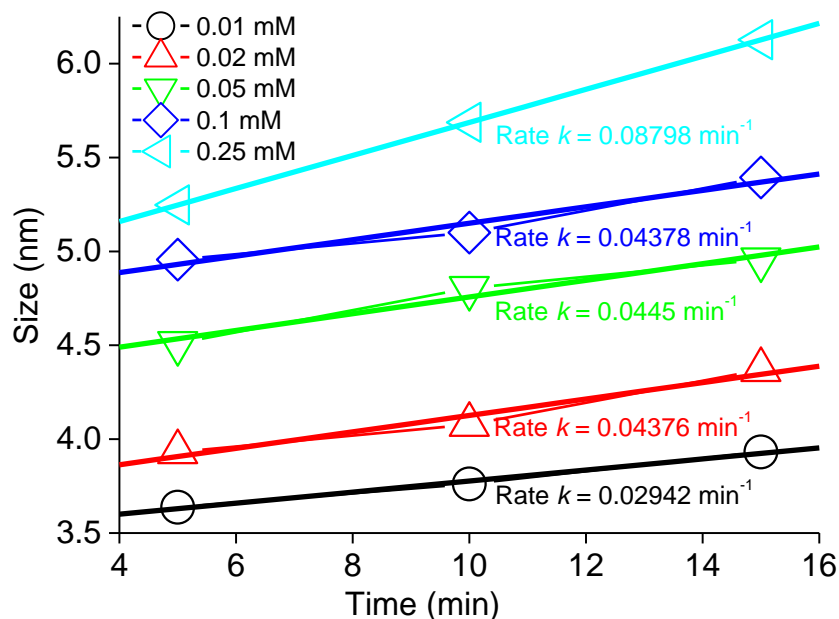
Figure S10. Initial rate kinetic analysis. Plot of ln[size (nm)] *vs.* time (min) for initial rate kinetic analysis on the formation of spherical particles at different initial concentrations of **(R)-NP(OH)₂** (0.01–0.25 mM) in DCM:hexane (1:2) mixture.
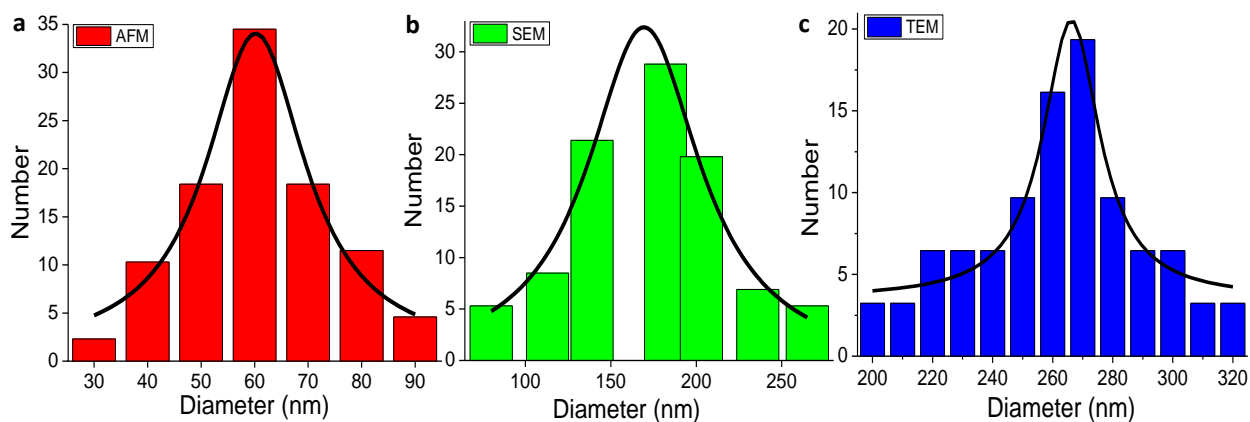

Figure S11. Particle size distribution of vesicular **(R)-NP(OH)₂** by AFM, SEM and TEM analysis. Histogram of the size distribution of **(R)-NP(OH)₂** spherical assemblies in DCM:hexane (1:2) mixture counted for 500 individual particles obtained from (a) AFM (c = 50 × 10⁻⁶ M); (b) SEM (c = 10 × 10⁻⁵ M) and (c) TEM images (c = 25 × 10⁻⁵ M) at different places of the sample.
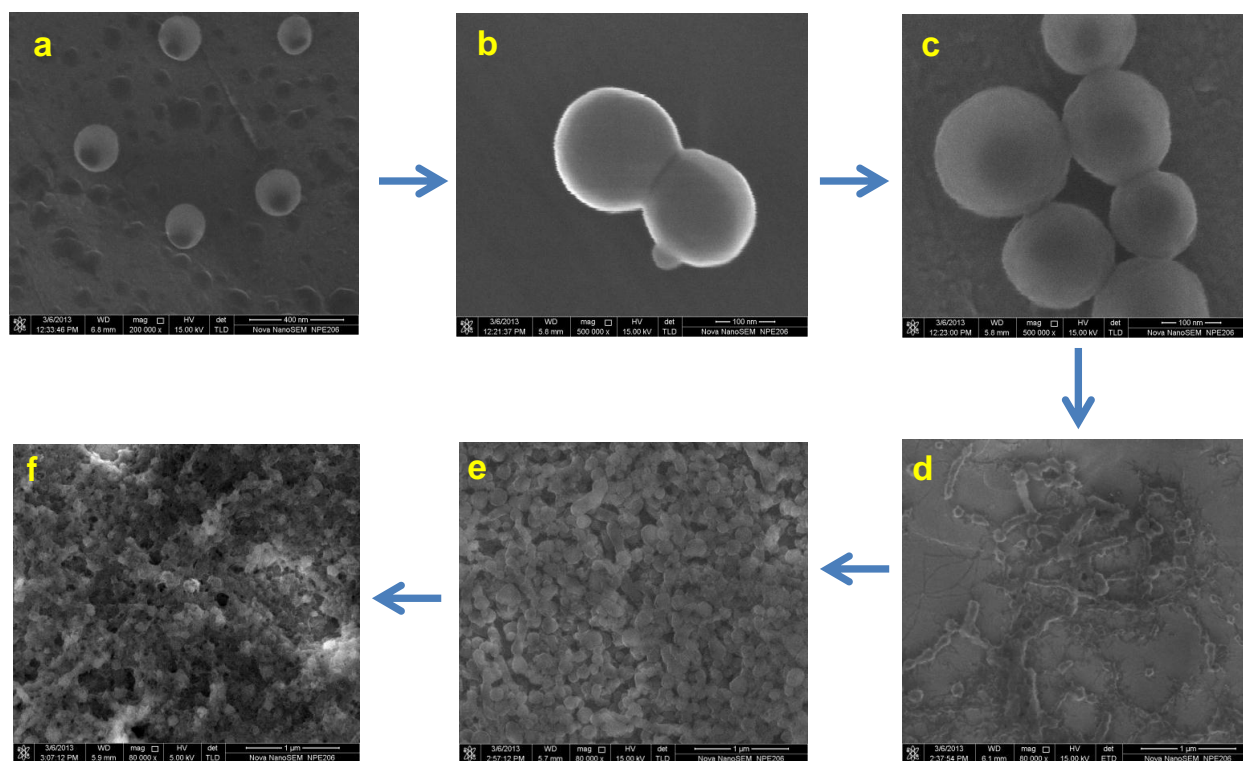
Figure S12. SEM imaging of evolution of the gel from vesicle. Concentration dependent SEM images of **(R)-NP(OH)₂** spherical assemblies in DCM:hexane (1:2) mixture at (a) 0.01 mM; (b) 0.02 mM; (c) 0.05 mM; (d) 0.1 mM; (e) 0.25 mM and (f) 0.5 mM of **(R)-NP(OH)₂**.
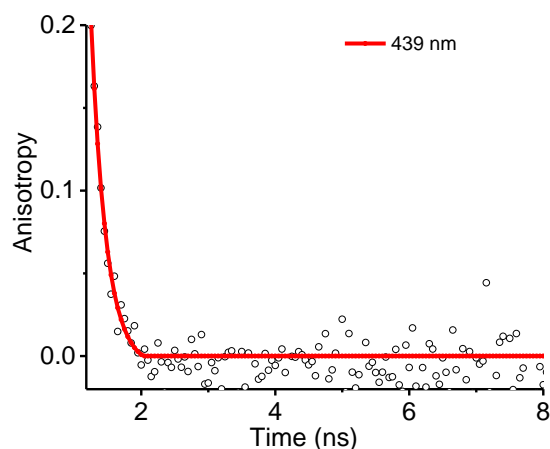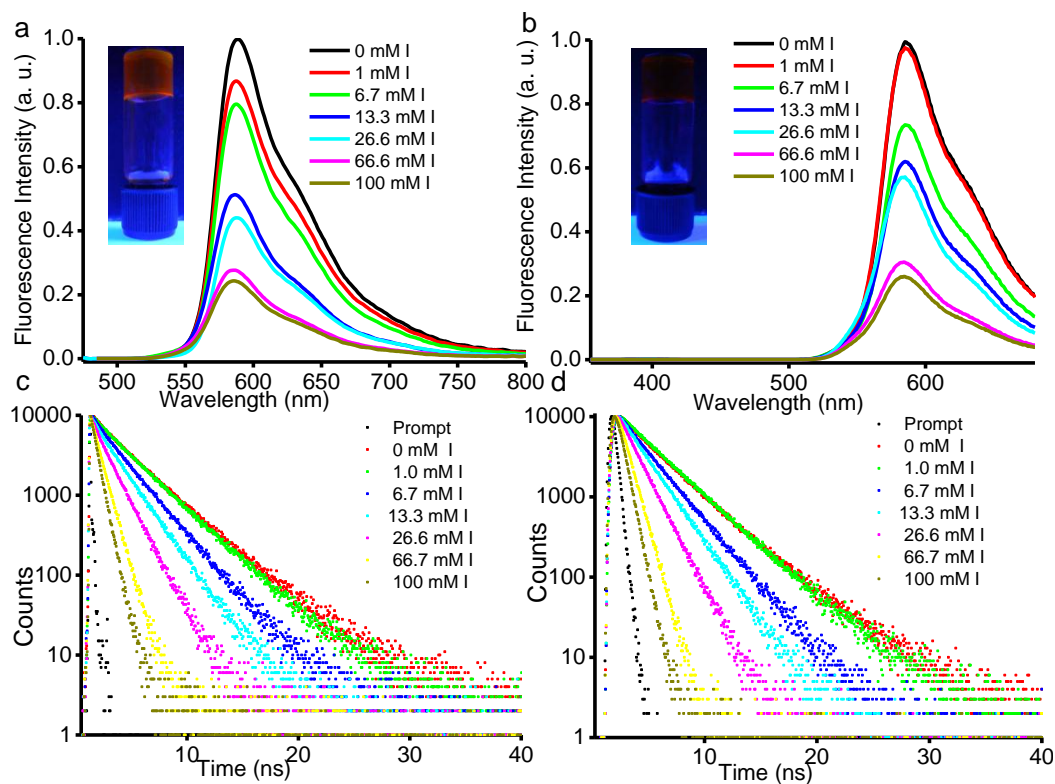

Figure S13. Fluorescent anisotropy of vesicular **(R)-NP(OH)₂** gel. Time-resolved fluorescence anisotropy decay of **(R)-NP(OH)₂** gel when excited at 439 nm and monitored at 580 nm. Concentration of **(R)-NP(OH)₂** in gel state is 1 mM (critical gelator concentration).
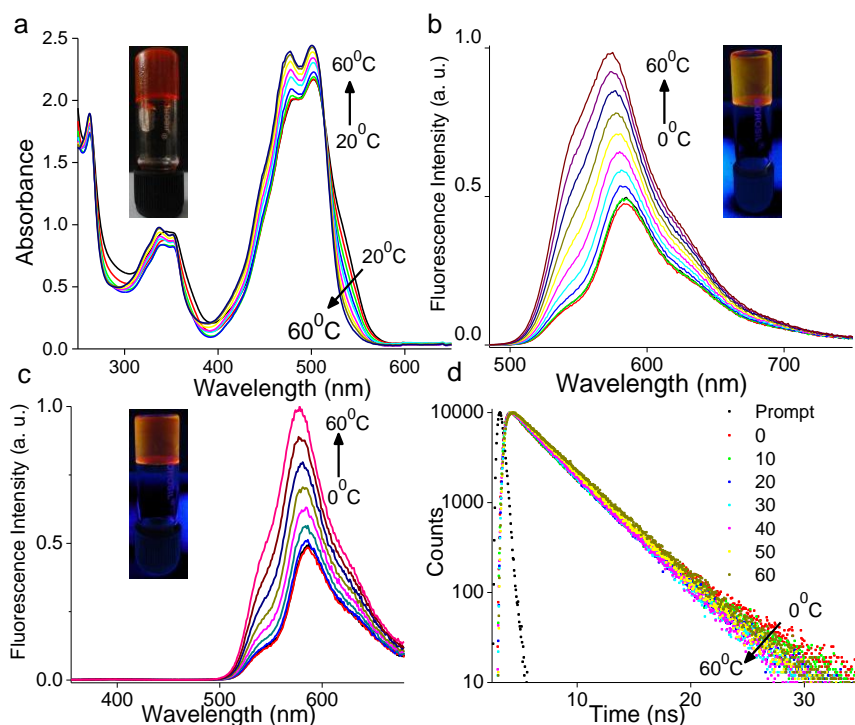
Figure S14. Thermodynamic stability of vesicular **(R)-NP(OH)₂** gel. Temperature dependent (a) UV–Vis; (b) fluorescence spectra when excited at 475 nm radiation; (c) fluorescence spectra when excited at 345 nm and (d) time-resolved fluorescence decay upon excitation at 340 nm and monitored at 580 nm. Arrows indicate the increase in temperature from 0–60°C. Inset shows the photographic image of **(R)**-**NP(OH)₂** gel in DCM:hexane (1:2) mixture under (a) visible light; (b) long-wavelength UV radiation and (c) short–wavelength UV radiation. Concentration of **(R)-NP(OH)₂** in gel state is 1 mM (critical gelator concentration).
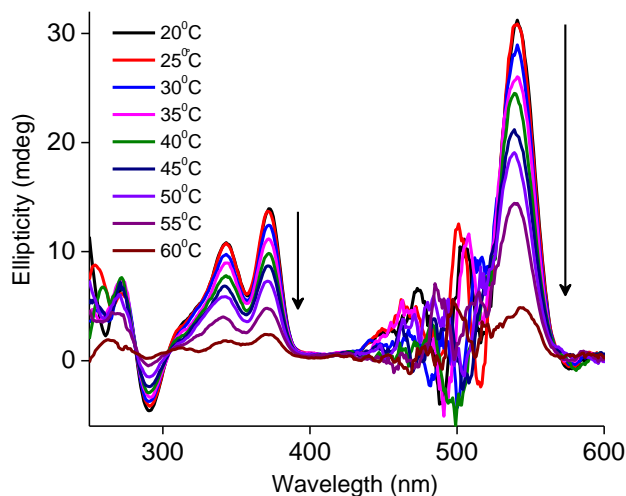

Figure S15. Temperature dependent chiroptical spectra of **(R)-NP(OH)₂** gel. Temperature-dependent circular dichroism spectra of representative **(R)-NP(OH)₂** gel in DCM:hexane (1:2). Concentration of **(R)-NP(OH)₂** in gel state is 1 mM (critical gelator concentration).

20

Figure S16. Steady-state and time-resolved fluorescence quenching of vesicular **(R)-NP(OH)$_2$** gel in the presence of indole. Indole **(I)** concentration dependent emission spectra of **(R)-NP(OH)$_2$** gel when excited at (a) 475 nm; (b) 345 nm; indole concentration dependent time-resolved fluorescence decay of **(R)-NP(OH)$_2$** gel when excited at (c) 439 nm and (d) 340 nm (emission monitored at 580 nm). Insets show the photographic image of **(R)-NP(OH)$_2$** + **I** co-gel in DCM:hexane (1:2) mixture under (a) long–wavelength UV radiation and (b) short–wavelength UV radiation. Concentration of **(R)-NP(OH)$_2$** in gel state is 1 mM (critical gelator concentration).
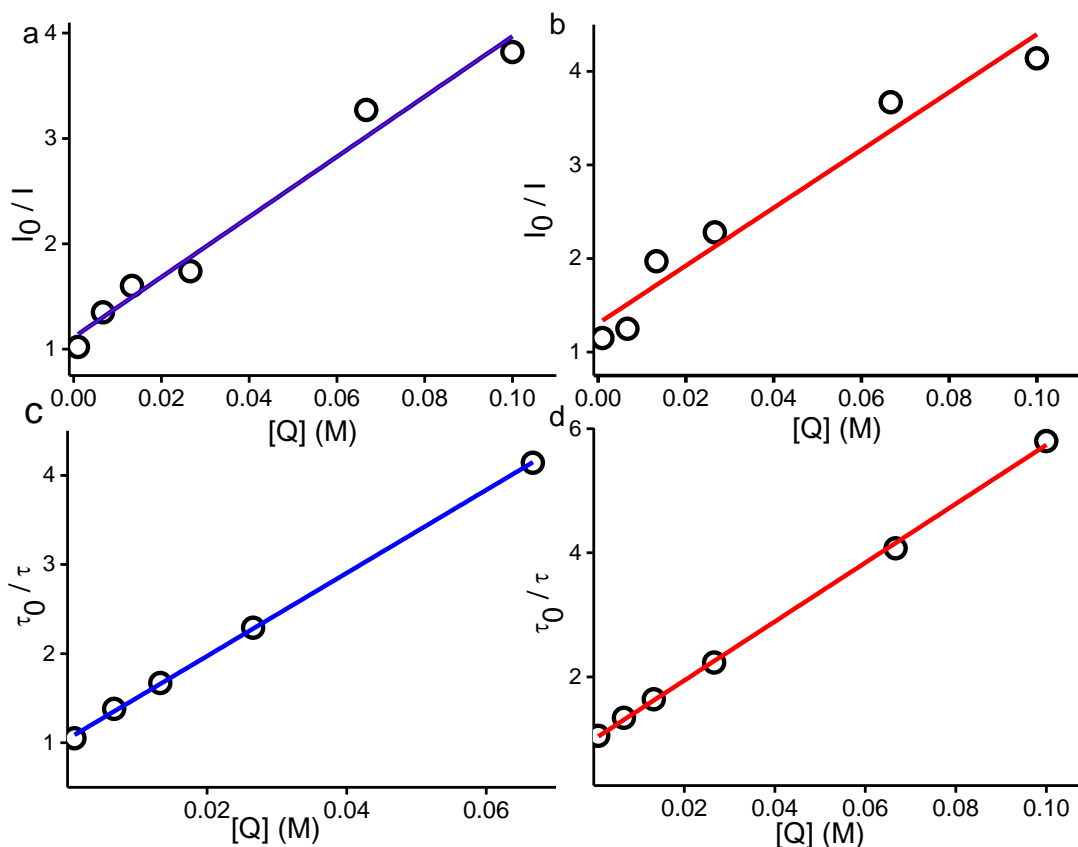
Figure S17. Stern-Volmer plots. Steady-state (when excited at (a) 345 nm and (b) 475 nm); and time-resolved (when excited at (c) 340 nm and (d) 439 nm (emission monitored at 580 nm))-based Stern–Volmer plot of **(R)-NP(OH)₂** gel with increase in concentration of indole. Concentration of **(R)-NP(OH)₂** in gel state is 1 mM (critical gelator concentration). In the case of 340 nm excitation the lifetime corresponding to 0.1 M concenrtaion is omited since measured lifetime is shorter than the resolution of the excitation source.
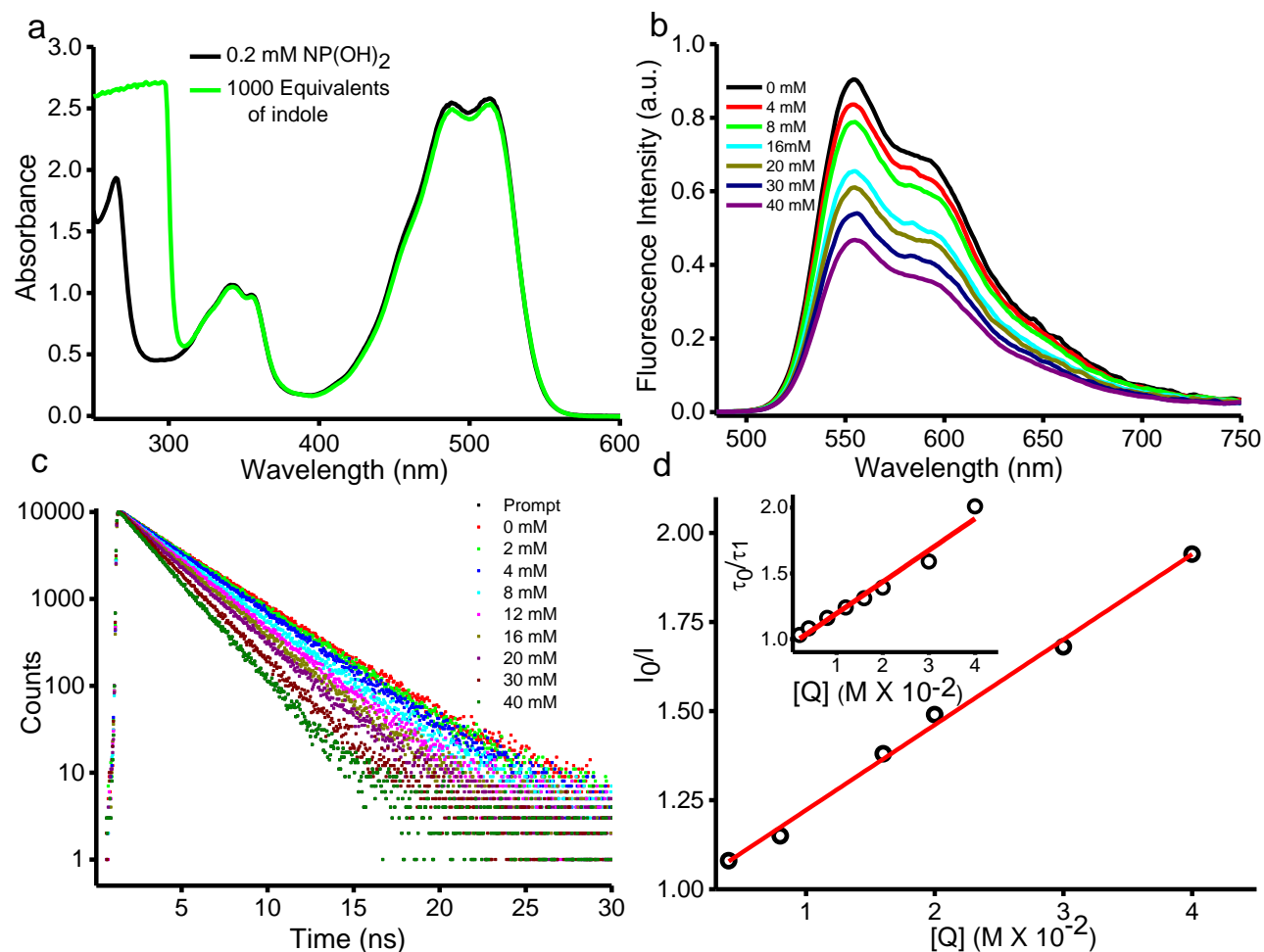
Figure S18. (a) Absorption spectra of 0.2 mM **(R)-NP(OH)$_2$** solution in the absence and presence of 1000 equivalents of indole; (b) indole **(I)** concentration dependent emission spectra of **(R)-NP(OH)$_2$** solution when excited at 475 nm; (c) indole concentration dependent time-resolved fluorescence decay of **(R)-NP(OH)$_2$** solution when excited at 475 nm (emission monitored at 580 nm); steady-state when excited at (d) 475 nm, inset of (d) shows time-resolved (when excited at 439 nm & monitored at 580 nm)-based Stern–Volmer plot of **(R)-NP(OH)$_2$** solution with increase in concentration of indole. Concentration of **(R)-NP(OH)$_2$** in solution is 8 µM for steady-state and time-solved fluorescence measurements.
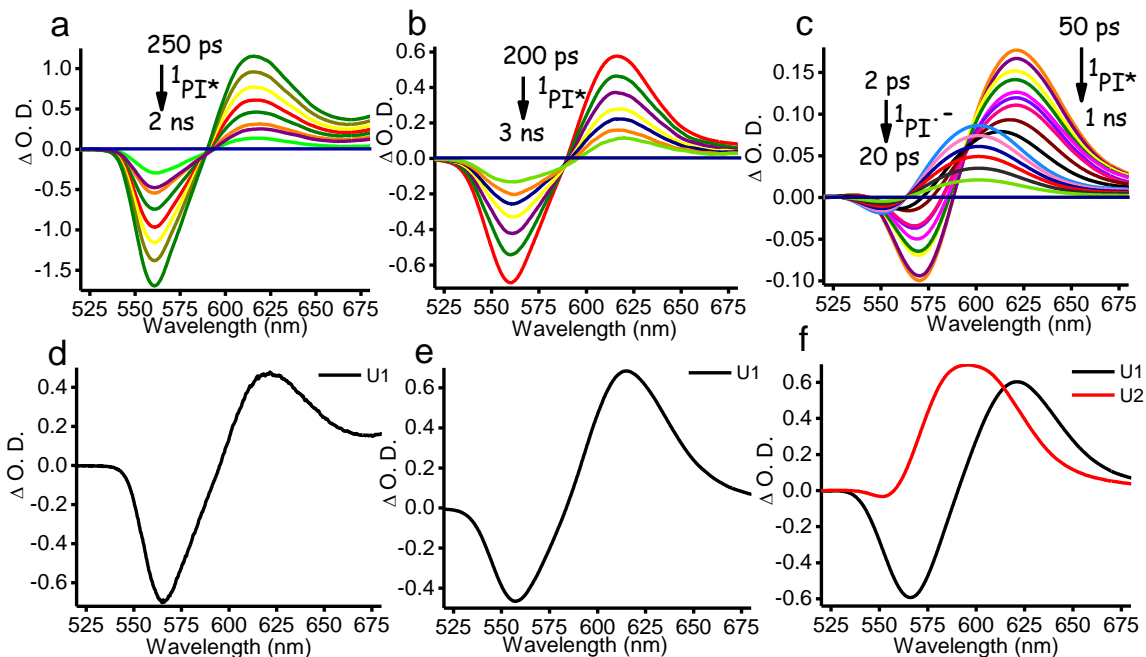
Figure S19. Femtosecond-transient absorption spectra of (**R**)-**NP(OH)₂** (a) solution (0.75 mM); (**R**)-**NP(OH)₂** solution (0.75 mM): Indole (b) 1:10; (c) 1:500 and right singular vectors obtained from SVD analysis of (**R**)-**NP(OH)₂** (d) solution (0.75 mM); (**R**)-**NP(OH)₂** solution (0.75 mM): Indole (e) 1:10 and (f) 1:500 respectively when excited at 390 nm.
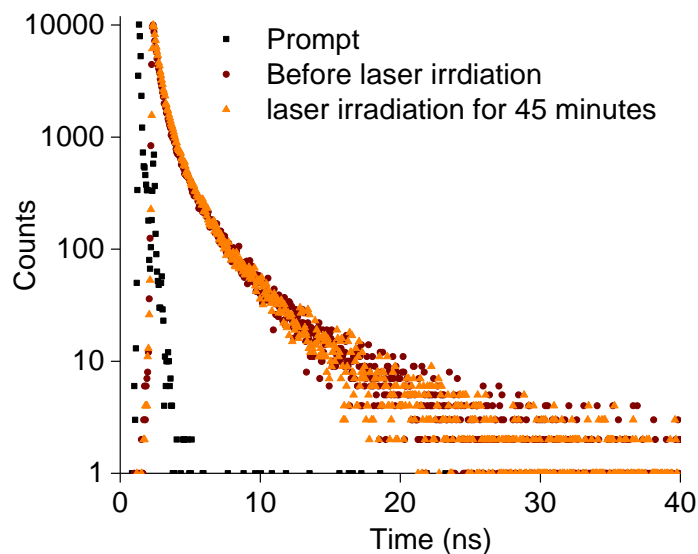
Figure S20. Effect of laser (3 µJ for 45 minutes) irradiation on the fluorescence lifetime of (**R**)-**NP(OH)₂** thin film upon excitation at 439 nm. Emission was collected at 580 nm.